# Low-Energy Ion-Induced Electron Emission from a MgO(100) Thin Film: The Role of the MgO-Substrate Interface

Y. T. Matulevich,[1] T. J. Vink,[2] and P. A. Zeijlmans van Emmichoven[1]
[1]*Debye Institute, Utrecht University, P.O. Box 80000, 3508 TA Utrecht, The Netherlands*
[2]*Philips Research Laboratories, Professor Holstlaan 4, 5656 AA Eindhoven, The Netherlands*

(Received 12 April 2002; published 1 October 2002)

We present a detailed study of the electron emission from a thin MgO(100) film on a Mo substrate, bombarded with slow $He^+$, $Ne^+$, and $Ar^+$ ions. Neither the high absolute number of emitted electrons per incoming ion nor the electron spectra can be due to Auger neutralization of the incoming ions at the MgO surface alone. Therefore, an additional mechanism is proposed: holes created in the MgO film are transported to the MgO-substrate interface where they give rise to an Auger neutralization process involving two electrons from the metal substrate conduction band.

DOI: 10.1103/PhysRevLett.89.167601 PACS numbers: 79.20.Rf, 34.70.+e

Electron emission from insulators under slow ion bombardment has received considerable attention in the last years [1–3]. One of the driving forces is the technological importance of insulating protective layers in plasma display panels (PDPs) [4]. The protective layer in a PDP determines the ion-induced secondary electron-emission coefficient and thus the driving voltage and power consumption. Presently MgO is used because of its high electron yield and high stability under ion bombardment. The study of the detailed processes leading to electron emission is also of fundamental interest. For slow ions incident on metal surfaces these processes are rather well established [5–7]. A typical example is Auger neutralization, in which a conduction electron is transferred to the projectile ground state of larger binding energy and the excess energy is transferred to another conduction electron that may be emitted from the metal. For insulators, the electron-emission processes and their relative importance are far less understood. The reason is clear: the target is a bad conductor and, without special precautions, the ions will charge up the surface. To avoid charging, thin layers of insulators grown on conducting substrates are often used.

In this Letter, we present results of experiments on the electron emission from a thin MgO(100) layer on a Mo substrate bombarded by slow ions and compare with simulations. The comparison clearly shows that Auger neutralization of the incoming ions at the MgO thin layer is not able to explain the experimental observations. We will show that the metallic substrate plays a very important role for the overall electron emission: the holes created in the MgO film are transported to the MgO-substrate interface, where they are neutralized by Auger neutralization.

The experiments were carried out in a UHV chamber at a background pressure of $5 \times 10^{-10}$ mbar. The thin MgO(100) layer was grown on a Mo(100) substrate by evaporating Mg in an oxygen atmosphere of $5 \times 10^{-7}$ mbar [8]. The substrate was kept at 250 °C during the evaporation process. To monitor the growth of the MgO layer and to check the film quality, low-energy ion scattering (LEIS) and ultraviolet photoelectron spectroscopy (UPS) measurements were carried out. The growth was finished as soon as any sign of the substrate had vanished, in LEIS as well as in UPS. This implies a film thickness of approximately 1–5 nm. The dependence of the scattered ion intensity on azimuthal angle clearly demonstrated that the MgO film had a (100) crystalline structure. In the UPS spectra two peaklike structures were observed that correspond to the MgO valence band formed by the $2p$ electrons of O. Our UPS spectra strongly resembled those reported in [9]. Only a very small amount of filled defect states was detected by the UPS measurements (the integrated intensity above the valence-band maximum amounts to approximately 2%–3% of the total spectral intensity).

Prior to the measurements the MgO(100) thin layer was annealed for 20 min at 400 °C to desorb water and hydroxyls from the surface [8]. The MgO(100) layer was then bombarded by 40 eV noble-gas ions incident at 40° with respect to the surface. The absolute numbers of emitted electrons per incoming ion ($\gamma$) were determined from the sample current and from the current of primary ions as measured in a Faraday cup: $\gamma(He^+) = 0.55 \pm 0.05$, $\gamma(Ne^+) = 0.41 \pm 0.04$, and $\gamma(Ar^+) = 0.10 \pm 0.01$. These $\gamma$ values are substantially higher than the ones reported in a recent summary [2], the main difference with our experiments being the use of much thicker films. We also measured the electron energy distributions. The results are shown in Fig. 1. To minimize the influence of the earth magnetic field on the low-energy part of the spectrum, a negative potential of $-7$ V was applied to the sample. The effect of this potential on ion energies and angles of incidence is not of any importance and the values given above have therefore not been corrected. The peaks at electron energies of 5.6 eV correspond to 0 eV electrons at the MgO surface. We found the peak position to be independent of the

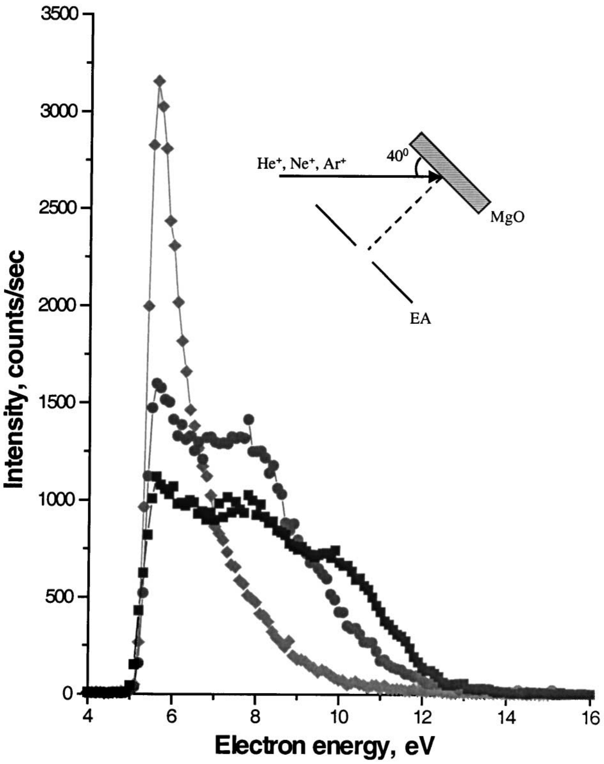

FIG. 1. Raw electron energy distributions, obtained with a 1.4 nA beam of 40 eV $Ar^+$ ions (◆), a 1.1 nA beam of 40 eV $Ne^+$ ions ( • ), and a 1.0 nA beam of 40 eV $He^+$ ions (■) incident on MgO(100) thin layer in the ⟨100⟩ direction at 40° with respect to the surface. The energy is given with respect to the vacuum level of the analyzer. Electrons were detected in the direction of the surface normal. During the measurements, the crystal was at room temperature. A potential difference of 7 V was applied between analyzer and crystal. In the inset a sketch of the experiment is shown. The first aperture of the energy analyzer is denoted by EA.

primary ion current, which implies that the MgO layer did not charge up. The peaks show up at somewhat lower energies than the applied acceleration voltage, because of the work-function difference between sample and analyzer. We also performed experiments with thicker films. For slightly thicker films, the spectra do not change significantly. For thicker films (of approximately 10–40 nm), we observed shifts of the low-energy peaks, indicating that the surface charges up. Here we will consider only the results obtained at the very thin MgO film. In Fig. 1, the high-energy tails of the spectra are shifted with respect to each other, which is characteristic for Auger neutralization and which is related to the differences in ionization potentials of the primary particles. By assuming a uniform electric field and a cosinelike angular distribution of emitted electrons, the measured energy distributions can easily be corrected for the acceleration voltage. In Fig. 2(a) the corrected experimental energy distributions are shown with, in the inset, the high-energy parts. It is remarkable that all three energy distributions extend up to approximately the same energy.

In the following we discuss the numerical simulations that we have performed. For the incidence conditions used, the trajectories of 500 incoming ions have been calculated. A slab of $16 \times 16 \times 4$ fixed ions was used with equal numbers of $Mg^{2+}$ and $O^{2-}$ ions. Using Hartree's atomic units, the total potential energy of the projectile-slab interaction $U$ can be written as

$$U = \sum_{i=1}^{N} U_i,$$

$$\text{with } U_i = U_i^{\text{Mol}} + U_i^{\text{Madelung}} + U_i^{\text{pol}} = U_i^{\text{Mol}} \pm \frac{2}{R_i} - \frac{\alpha_i}{\varepsilon R_i^4}, \qquad (1)$$

where $U_i$ is the interaction pair potential energy, $N$ is the number of target ions, $U_i^{\text{Mol}}$ is the Molière potential energy, $R_i$ is the distance between the projectile and the $i$th target ion, $\alpha_i$ is the polarizability of the $i$th target ion [$\alpha(Mg^{2+}) = 0.094$ Å$^3$ and $\alpha(O^{2-}) = 3.88$ Å$^3$ [10]], and $\varepsilon$ is the dielectric constant. The dielectric constant $\varepsilon$ accounts for the screening of the electric field of the primary ion. To test the quality of the potentials used, for the $He^+$-$Mg^{2+}$ system we made a comparison with

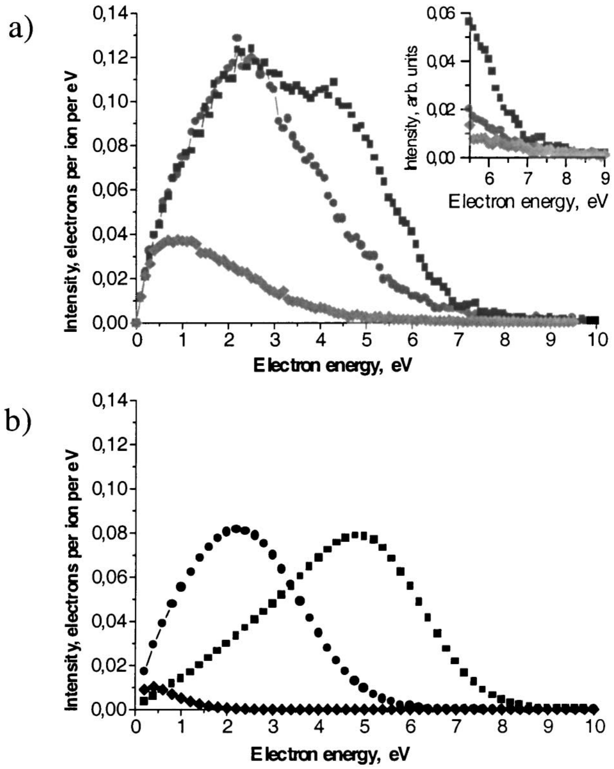

FIG. 2. (a) Same as Fig. 1, but after correction for the transmission function of the energy analyzer and for the 7 V acceleration. The energy is given with respect to the vacuum level of the sample. The area under each curve has been taken equal to the corresponding measured value for $\gamma$. The high-energy tails of the spectra are shown in the inset (intensity of $Ar^+$ spectrum multiplied by 5). (b) Simulated electron energy distributions (same conditions as used in the experiments).

potentials calculated using density functional theory [11] and found very good agreement. Using the total potential energy $U$, the projectile trajectories have been calculated numerically.

Along each trajectory, neutralization of the ion via Auger neutralization (AN) was considered. Because of the wide band gap of MgO (at the surface 6.7 eV [12]), resonant processes into excited states are not possible. Electron wave functions of the valence band in MgO are strongly localized on anion sites. Two electrons involved in AN can be taken from the same anion site (on site or two-centered AN) or from different sites (off site or three-centered AN). Two-centered AN may be energetically unfavorable: the *effective* binding energy for the removal of two electrons from the same site may be significantly larger than twice the binding energy for the removal of one electron, because of the presence of two holes in the final state and electron correlation effects [13,14]. Three-centered AN was therefore recently considered for the neutralization of $\mathrm{Ne}^+$ on LiF(001) [15]. We will first show that for MgO two-centered AN is energetically possible. AN is considered to be a two-step process, both steps creating positive holes on the same $\mathrm{O}^{2-}$ site. The unperturbed MgO is used as a reference point with the potential energy $W^0$ taken to be 0. The binding energies of the first and second electrons are given by the potential energy differences $W^{1\mathrm{h}} - W^0$ and $W^{2\mathrm{h}} - W^{1\mathrm{h}}$, respectively, with [16]

$$W^{1\mathrm{h}} = U_{\mathrm{hole}}^{\mathrm{Madelung}} + U_{\mathrm{hole}}^{\mathrm{pol}} + \Delta W_1^{\mathrm{free}}, \tag{2}$$

$$W^{2\mathrm{h}} = 2\,U_{\mathrm{hole}}^{\mathrm{Madelung}} + 4\,U_{\mathrm{hole}}^{\mathrm{pol}} + \Delta W_1^{\mathrm{free}} + \Delta W_2^{\mathrm{free}}. \tag{3}$$

$U_{\mathrm{hole}}^{\mathrm{Madelung}}$ is the potential energy of a hole in the Madelung potential, $U_{\mathrm{hole}}^{\mathrm{pol}}$ is the potential energy due to the polarization of MgO by the hole, and $\Delta W_1^{\mathrm{free}} = -9$ eV and $\Delta W_2^{\mathrm{free}} = 1.4$ eV are the electron affinities for $\mathrm{O}^-$ and O in vacuum, respectively [10,17]. From our slab calculation we found $U_{\mathrm{hole}}^{\mathrm{Madelung}} = 21.7$ eV for a positive hole at an $\mathrm{O}^{2-}$ site. Using $E_b = W^{1\mathrm{h}} - W^0 = 8.3$ eV, which corresponds to the binding energy at the maximum intensity in the density of states (DOS) as determined by UPS, and solving Eqs. (2) and (3), we get $(W^{2\mathrm{h}} - W^{1\mathrm{h}}) - (W^{1\mathrm{h}} - W^0) = 1.6$ eV. This value, corresponding to the extra binding energy for removal of the second electron, is small in comparison with the MgO valence-band width of 6.5 eV [9] and may even be further reduced by screening by the substrate [16]. We therefore conclude that two-centered AN is energetically possible and, since the overlap of wave functions of these electrons is larger than in a three-centered AN, we expect the transition rates to be significantly larger. We have therefore considered only two-centered AN, with the electron spectra constructed as the convolution of the one-electron DOS and the one-electron DOS shifted by 1.6 eV. For the DOS we used a fit of two Gaussians to our UPS spectrum. The final electron energies are further determined by the local ionization potential (IP) of the primary ion: $\mathrm{IP} = \mathrm{IP}_0 + U^{\mathrm{Madelung}} + U^{\mathrm{pol}} + U^{\mathrm{Mol}}$, with $\mathrm{IP}_0$ the ionization potential in vacuum.

The transition rate for AN was approximated by [5,6,9]

$$G = G_0 \exp(-a\,r), \qquad \text{with } a = 2\left(\frac{1}{\sqrt{2E_b}} + \frac{1}{\sqrt{2\mathrm{IP}_0}}\right)^{-1}, \tag{4}$$

with $G_0$ a fitting parameter, $r$ the distance between the primary ion and the nearest $\mathrm{O}^{2-}$ ion, and $E_b$ and $\mathrm{IP}_0$ as above. The transition rate was corrected for the number of available initial states that may give rise to electron emission. The rate equation for Auger neutralization was solved numerically along the trajectories of the projectiles. The surface barrier $E_s$ for an escaping electron was taken to be equal to the electron affinity of MgO (0.5 eV [12]).

The electron spectra can now be evaluated. The model has two fitting parameters, i.e., $G_0$ and $\varepsilon$. $\varepsilon$ is mainly of importance for the shift of the IP of the primary ions and therefore directly has an effect on the energy of the emitted electrons. Considering the time scale for the AN process, the value of $\varepsilon$ should be in the range of unity up to the optic dielectric constant $\varepsilon = 3$ [10]. To determine values for the parameters, the shape and maximum position of the electron energy distribution from $\mathrm{Ne}^+$ were fitted ($G_0 = 1.9 \times 10^{17}\ \mathrm{sec}^{-1}$ and $\varepsilon = 2.5$). The result is shown in Fig. 2(b). Also shown are the simulated results obtained for $\mathrm{He}^+$ and $\mathrm{Ar}^+$ primary ions using the same fitting parameters. For $\mathrm{He}^+$, compared to the experiments, intensity seems to be missing at the lower energies. The measured and calculated energy distributions for $\mathrm{Ar}^+$ also significantly differ. Whereas in the simulations the energies of emitted electrons extend up to only approximately 2 eV, in the experiments they extend much further up to even 7 or 8 eV. We have tried to remove these discrepancies between experiments and simulations by variation of the free parameters, but found this to be impossible. Also, AN, in which defects present in MgO are involved, we do not consider to be very important: our UPS measurements clearly show only a very weak population of defect states. Our results therefore strongly suggest another mechanism for electron emission is active. We do know that, somehow, the holes produced in the MgO valence band have to be removed, since we have found that the surface does not charge up during ion bombardment. We propose that removal of the holes is related to the emission of electrons according to the following scenario: holes are created in the valence band via Auger neutralization at the MgO film for $\mathrm{He}^+$, for $\mathrm{Ne}^+$, and, to a lesser extent, for $\mathrm{Ar}^+$. For $\mathrm{Ar}^+$, additional holes are created via resonant neutralization (RN), since the ionization level lies energetically close to the bottom of the MgO valence band (see Fig. 3). The holes start to move through the thin MgO layer and, sooner or later, reach the Mo substrate. Since the film is very thin, it is likely that the binding energies of the holes do not

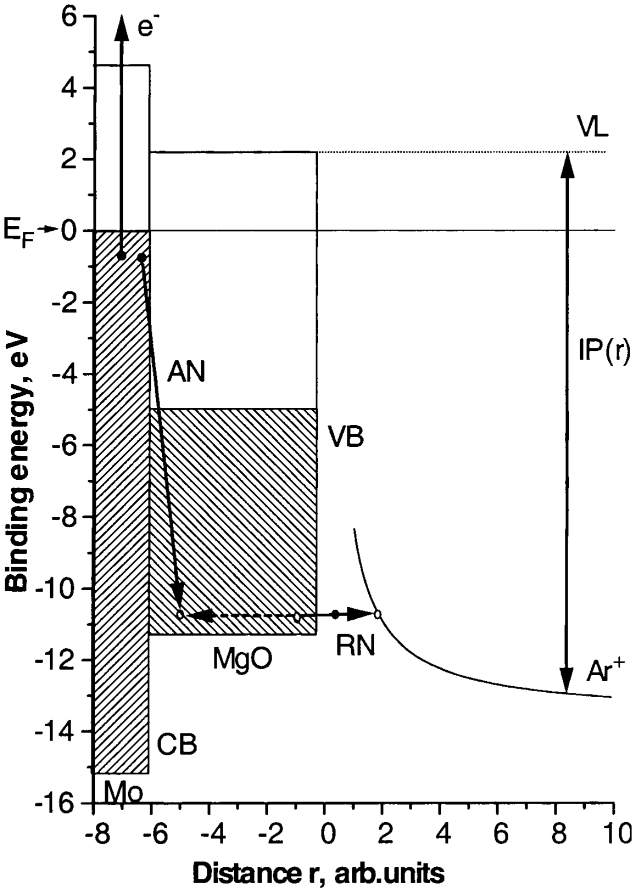

FIG. 3. Schematic energy-level diagram for resonant neutralization (RN) of an $Ar^+$ ion in front of a MgO thin film. The width of the MgO band was taken from our UPS results (see also [9]). The hole created in the valence band (VB) is transported to the substrate, where it is removed by Auger neutralization (AN), involving two electrons from the substrate conduction band (CB). VL denotes the vacuum level of MgO.

drastically change during transport. The holes are neutralized close to the Mo substrate, either via AN or via RN in which electron(s) from the conduction band of the substrate are involved. Although we cannot exclude RN, we will show in the following that we have strong arguments that AN of the holes at the substrate significantly contributes to the overall electron emission. In case of an AN, the excited electron may be directed towards vacuum. Since the film is thin and the mean free path of low-energy electrons in MgO is large, the probability for transport of an electron through the film and emission into vacuum is large. From a simple energy consideration (see Fig. 3), it follows directly that this leads to the emission of electrons with energies from 0 to 9 eV(with respect to the vacuum level of MgO). These electrons are responsible for the high-energy part of the $Ar^+$-induced spectrum and for the low-energy part of the $He^+$-induced spectrum. This interesting process explains why the measured electron energy distributions extend up to approximately the same maximum energy [see inset of Fig. 2(a)], as well as why the experimentally determined $\gamma$ values are so high. Finally, it should be noted that the measured spectrum and $\gamma$ value for $Ar^+$ are close to what has been measured by Hagstrum for $Ar^+$ directly incident on a Mo surface: he measured electrons with energies up to about 6 eV and a $\gamma$ value of 0.12 [18]. Since in the MgO experiments the substrate was not directly "visible" for the primary ions, as we have shown by LEIS, we consider this resemblance as extra strong proof for the proposed (indirect) process.

In conclusion, we have presented results of the experimental and theoretical studies of the electron emission from a thin MgO(100) layer bombarded by noble-gas ions. Our results demonstrate that two processes contribute to the total electron yield: Auger neutralization of an incoming ion at the MgO surface and Auger neutralization of a valence-band hole at the MgO-substrate interface. This substrate effect will not occur only for the presently studied interface. By choosing an appropriate film-substrate combination, the ion-induced secondary electron-emission coefficient may be increased further. This opens new perspectives for the development of plasma display panels operating at lower driving voltages.

The authors thank L. F. Feiner for useful discussions. This work was performed as part of the program of the "Stichting voor Fundamenteel Onderzoek der Materie (FOM)," with financial support from the "Nederlandse Organisatie voor Wetenschappelijk Onderzoek (NWO)."

---

[1] E. H. Choi *et al.*, Jpn. J. Appl. Phys. **37**, 7015 (1998).
[2] Y. Motoyama *et al.*, IEEE Trans. Electron Devices **48**, 1568 (2001).
[3] M. Ishimoto *et al.*, in *Proceedings of the 7th International Display Workshop* (Society for Information Display, Japan, 2000), p. 683.
[4] L. F. Weber, in *Flat-Panel Displays and CRTs*, edited by L. E. Tannas, Jr. (Van Nostrand Reinhold, New York, 1985), Chap. 10.
[5] H. D. Hagstrum, Phys. Rev. **96**, 336 (1954).
[6] B. van Someren *et al.*, Phys. Rev. A **61**, 022902 (2000).
[7] V. Kempter, Comments At. Mol. Phys. **34**, 11 (1998).
[8] Ming-Cheng Wu *et al.*, J. Chem. Phys. **96**, 3892 (1992).
[9] D. Ochs *et al.*, Surf. Sci. **365**, 557 (1996).
[10] *Handbook of Chemistry and Physics*, edited by D. R. Lide (CRC Press, New York, 2000).
[11] A. Arnau and M. Peñalba (private communication).
[12] P. Sushko *et al.*, Surf. Sci. **450**, 153 (2000).
[13] G. A. Sawatsky, Phys. Rev. Lett. **39**, 504 (1977).
[14] A. Marini and M. Cini, Phys. Rev. B **60**, 11 391 (1999).
[15] H. Khemliche *et al.*, Phys. Rev. Lett. **86**, 5699 (2001).
[16] S. Altieri *et al.*, Phys. Rev. B **59**, R2517 (1999).
[17] B.V. King and F. Freund, Phys. Rev. B **29**, 5814 (1984).
[18] H. D. Hagstrum, Phys. Rev. **104**, 672 (1956).